Eta and Etaprime Photoproduction with EtaMAID

Lothar Tiator for the Mainz-Tuzla-Zagreb collaboration

SFB 1044

THE LOW-ENERGY FRONTIER OF THE STANDARD MODEL

PWA 2019, Mainz, 18-21 February

MTZ collaboration on γ,η γ,η' and Regge models

Mainz: Victor Kashevarov, Michael Ostrick, Misha Gorchtein, Kirill Nikonov, L.T.

Tuzla: Jugoslav Stahov, Hedim Osmanovic, Mirza Hadzimehmedovic, Rifat Omerovic

Zagreb: Alfred Svarc

recent publications:

Eta and Etaprime Photoproduction on the Nucleon with the Isobar Model EtaMAID2018
EPJ A54 (2018) 210

Role of angle-dependent phase rotations of reaction amplitudes in *η* photoproduction on protons, **PR C98 (2018) 045206**

Fixed-t analyticity as a constraint in single-energy partial-wave analyses of meson photoproduction reactions, **PR C97 (2018) 015207**

short history of EtaMAID

2000: isobar model with 7 N* resonances and t-channel ρ,ω pole contributions

2003: isobar model with 7 N* resonances and t-channel ρ,ω Regge trajectories

2007: search for narrow pentaquark state N(1685) in $\gamma n \to \eta n$

after 2007 a lot of new measurements were performed at:

MAMI, ELSA, JLAB

with high statistics and beam-target polarization techniques

2017/2018: EtaMAID update of 4 coupled channels: ηp, ηn, $\eta' p$, $\eta' n$

with up to 20 N* resonances and Regge phenomenology

photoproduction amplitudes in an isobar model

$$t_\alpha(W) = t_\alpha^{Bgr}(W) + t_\alpha^{Res}(W)$$

$\alpha = \alpha(\,L,\ J,\ I,\ E/M\,)$: set of partial wave quantum numbers

t_α^{Bgr} : Born $+\,t$-channel vector and axial-vector exchanges

Born terms

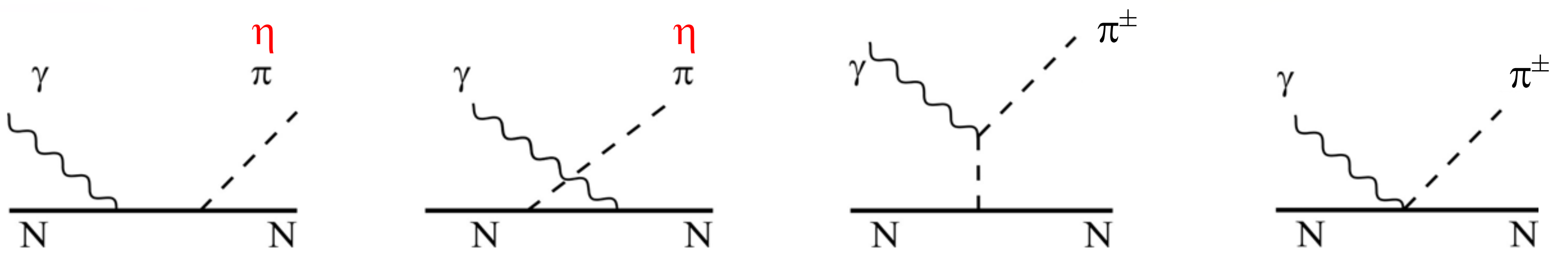

Born terms play a very different role in pseudoscalar photoproduction:

- very important for γ,π with well-known coupling constant ≈ 14
- small for γ,η and γ,η' with coupling constants < 0.1
- important for γ,K with practically unknown coupling constants

t-channel exchanges (single poles, Regge poles and Regge cuts)

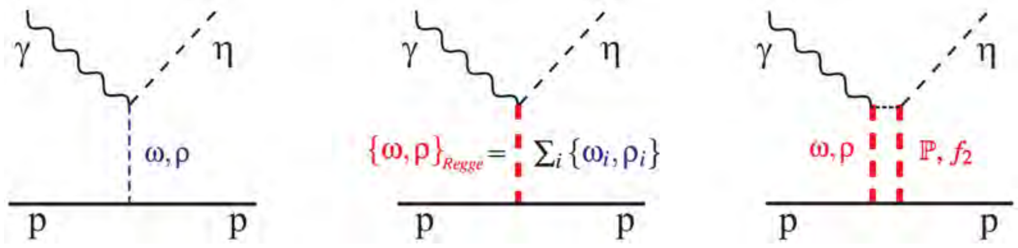

single poles   Regge poles   Regge cuts

Regge trajectories for: ω, ρ, ϕ, b_1, h_1

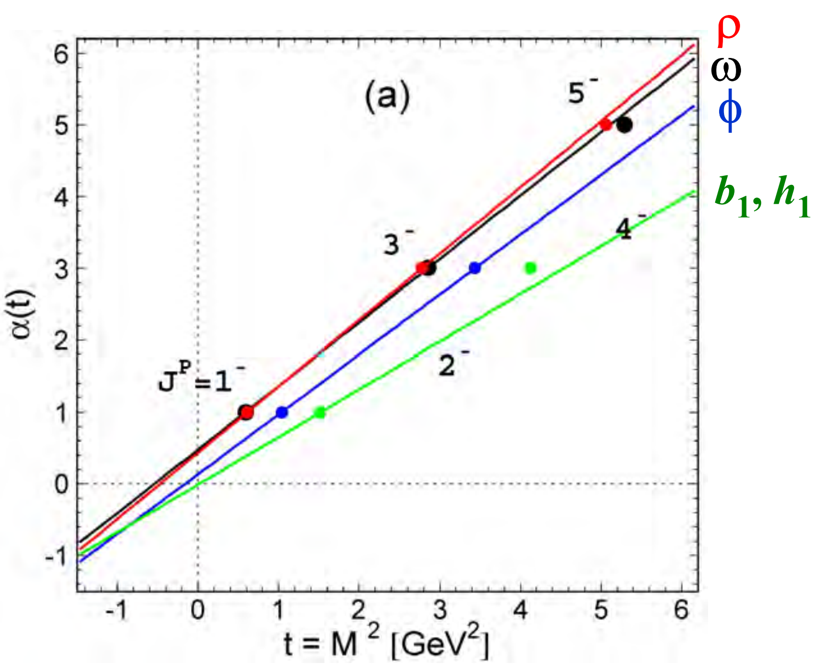

Regge trajectories for: f_2, P and cuts

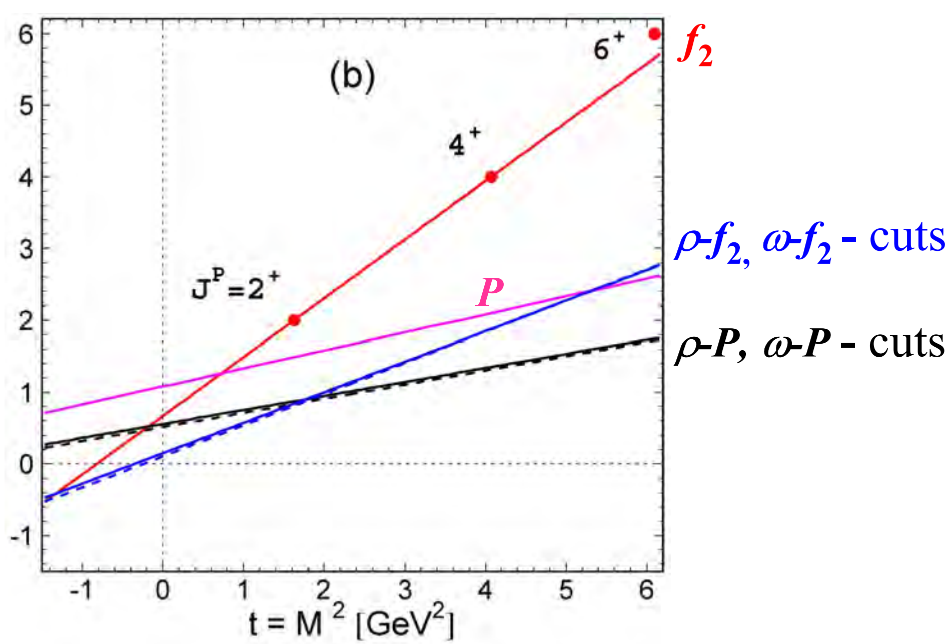

diff cross sections and beam asymmetry for γ,η at high energy

V. Kashevarov, M. Ostrick, L. Tiator , Phys. Rev. C**96** (2017) 045207

comparison with different Regge models —— our favoured Regge-cut model

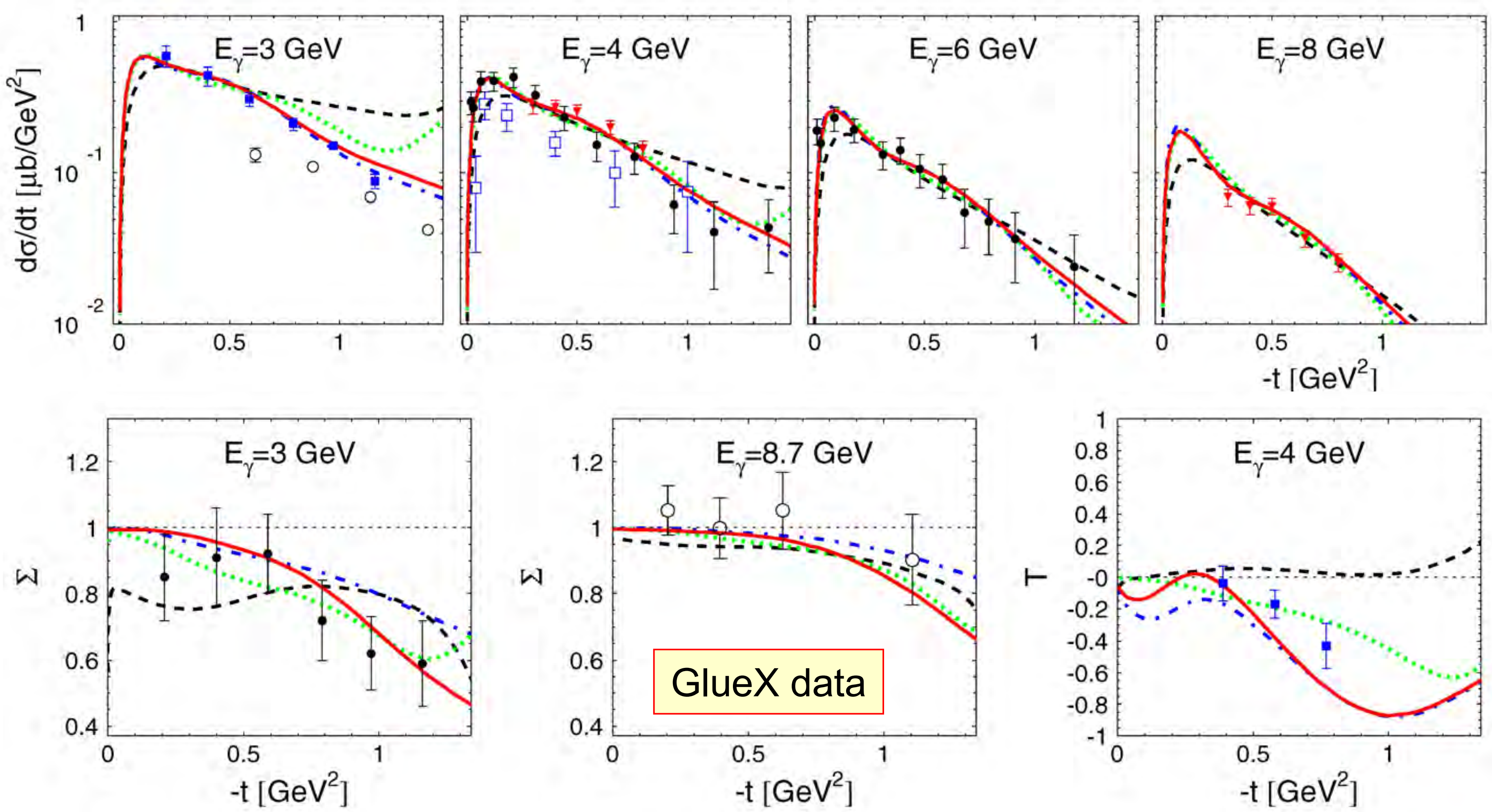

photoproduction amplitudes

$$t_\alpha(W) = t_\alpha^{Bgr}(W) + t_\alpha^{Res}(W)$$

t_α^{Bgr} : Born $+\,t$-channel vector and axial-vector exchanges

t_α^{Res} : $\sum_{i=1}^{n}\{\text{Breit-Wigner resonances } N,\Delta\}$

MAID2007 (γ,π) : $2\,S_{11}$, for all other channels only 1 resonance N and Δ

EtaMAID2018 (γ,η) : $4\,P_{11}$, $3\,S_{11}$, $4\,D_{13}$, … only N no Δ

problems:

- unitarity (Watson‘s theorem, coupled channels !)
- fixed-*t* analyticity (dispersion relations !)
- duality (problematic with Regge models !)

quark-hadron duality

from quark-hadron duality it is known:

sum over all s-channel resonances is equivalent to sum over all t-channel resonances

therefore: keeping both leads to double counting

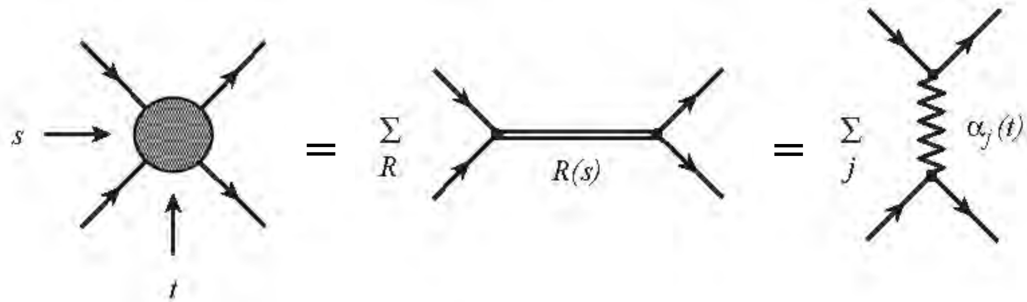

$$M = \sum_{i=1}^{\infty} M_s^{Res_i} = \sum_{i=1}^{\infty} M_t^{Res_i} = \sum_{i=1}^{N} M_s^{Res_i} + \left[\sum_{i=1}^{\infty} M_t^{Res_i} - \sum_{i=1}^{N} M_s^{Res_i} \right]$$

$$\approx \sum_{i=1}^{N} M_s^{Res_i} + M^{Regge} \cdot F_d(W)$$

: our approach

modelling the background

- Born
- Born + *t*-channel poles
- Born + Regge (RPR models)
- Born + Regge – s, p, d, f partial waves
- Born + Regge $*$ damping factor $f_d(\mathrm{W})$: our approach

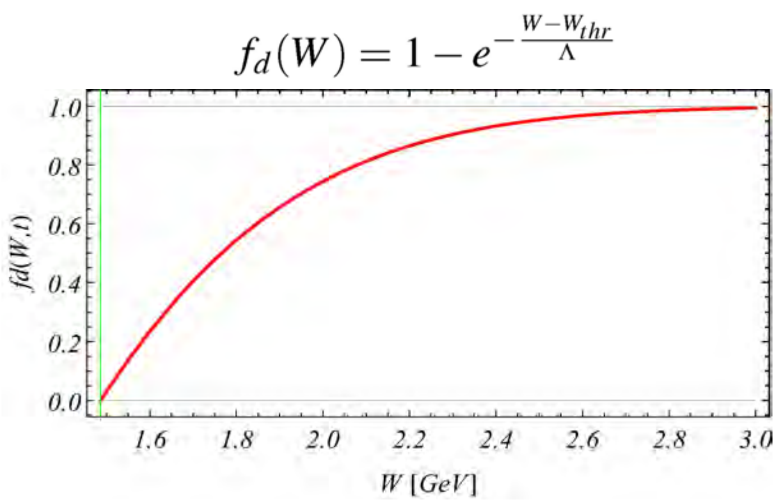

alternative approach: Finite Energy Sum Rules

unitarity aspects

the Unitary Isobar Model MAID for pion production

$$t^{\alpha}_{\gamma,\pi} = v^{\alpha}_{\gamma,\pi}(Born + \omega, \rho)\;(1 + i\,t^{\alpha}_{\pi,\pi})$$

K-matrix unitarization of background

$$+\; t^{\alpha}_{\gamma,\pi}(Resonances)\; e^{i\,\Phi(W)}$$

unitarization phase
determined by the Watson theorem, below 2π threshold
relaxed above 2π threshold

unitarity aspects

For eta production we don‘t have such a powerful constraint,
in previous versions EtaMAID 2000-2017 we simply ignored this phase.
In the new EtaMAID2018 version we use this phase as a free parameter.

$$t^{\alpha}_{\gamma,\eta}(W) = t^{\alpha,Born}_{\gamma,\eta}(W) + t^{\alpha,VM(Regge)}_{\gamma,\eta}(W) \cdot F_d(W)$$

$$+ \sum_{j=1}^{N_\alpha} t^{\alpha,BW,j}_{\gamma,\eta}(W) \cdot e^{i\Phi_j}$$

phenomenological phase
taken as a free parameter

Resonance excitations

isospin conservation:
in πN and $K\Sigma$ N* and Δ can be excited
in ηN, η'N and $K\Lambda$ only N* are possible

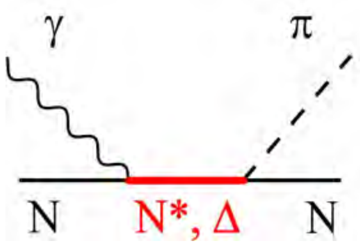

in s channel:
N*,Δ can be excited on shell

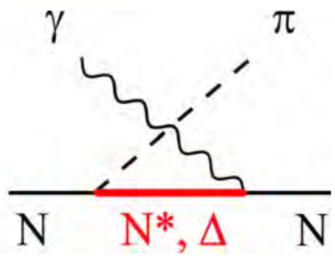

in u channel:
N*,Δ are off-shell

therefore, crossing symmetry is violated in any case
the u channel acts more like a background and can be absorbed by other bg contributions

crossing symmetry can be restored with fixed-t dispersion relations

Breit-Wigner ansatz for s-channel resonance excitations:

$$\mathcal{M}_{\ell\pm}(W) = \bar{\mathcal{M}}_{\ell\pm} f_{\gamma N}(W) \frac{M_R \Gamma_{\text{tot}}(W)}{M_R^2 - W^2 - i M_R \Gamma_{\text{tot}}(W)} f_{\pi N}(W) C_{\pi N}$$

$$f_{\pi N}(W) = \zeta_{\pi N} \left[\frac{1}{(2J+1)\pi} \frac{k}{q} \frac{M_N}{W} \frac{\Gamma_{\pi N}(W)}{\Gamma_{\text{tot}}(W)^2} \right]^{1/2}$$

$$f_{\gamma N}(W) = \left(\frac{k}{k_R}\right)^2 \left(\frac{X^2 + k_R^2}{X^2 + k^2}\right)^2$$

$C_{\pi N}$ is an isospin factor:

$$C_{\pi N} = \begin{cases} -1/\sqrt{3} & : \quad I = 1/2 \\ \sqrt{3/2} & : \quad I = 3/2 \end{cases}$$

for η and η' production:

$$C_{\eta N} = C_{\eta' N} = -1$$

$\zeta_{\pi N}$ is a relative phase
of an individual resonance:

$$\zeta_{\pi N} = 1,\ \zeta_{\eta N} = \pm 1,\ \zeta_{\eta' N} = \pm 1$$

energy-dependent width

The width of a Breit-Wigner resonance must be energy dependent.
Without the energy dependence, it is just a pole Ansatz
and works only in a narrow region around an isolated resonance, very bad for baryons.

The following Ansatz provides a correct threshold behavior.
At the resonance position $W = M_R$ it is normalized to the full width.
At high energy the Ansatz is more flexible and model dependent.

Threshold energies in MeV of various N^* decay channels

πN	$\pi\pi N$	ηN	$K\Lambda$	$K\Sigma$	ωN	$\eta' N$
1077.84	1217.41	1486.13	1609.36	1686.32	1720.92	1896.05

$$\Gamma_{\text{tot}}(W) = \Gamma_{\pi N}(W) + \Gamma_{\pi\pi N}(W) + \Gamma_{\eta N}(W) + \Gamma_{K\Lambda}(W) + \cdots$$

$$\begin{aligned}
\Gamma_{\pi N}(W) &= \beta_{\pi N}\,\Gamma_R \left(\frac{q_\pi}{q_{\pi,R}}\right)^{2\ell+1} \left(\frac{X^2+q_{\pi,R}^2}{X^2+q_\pi^2}\right)^{\ell} \frac{M_R}{W} \\
\Gamma_{\eta N}(W) &= \beta_{\eta N}\,\Gamma_R \left(\frac{q_\eta}{q_{\eta,R}}\right)^{2\ell+1} \left(\frac{X^2+q_{\eta,R}^2}{X^2+q_\eta^2}\right)^{\ell} \frac{M_R}{W} \\
&\vdots \\
\Gamma_{\pi\pi N}(W) &= (1-\beta_{\pi N}-\beta_{\eta N}-\cdots)\,\Gamma_R \left(\frac{q_{2\pi}}{q_{2\pi,R}}\right)^{2\ell+4} \left(\frac{X^2+q_{2\pi,R}^2}{X^2+q_{2\pi}^2}\right)^{\ell+2}
\end{aligned}$$

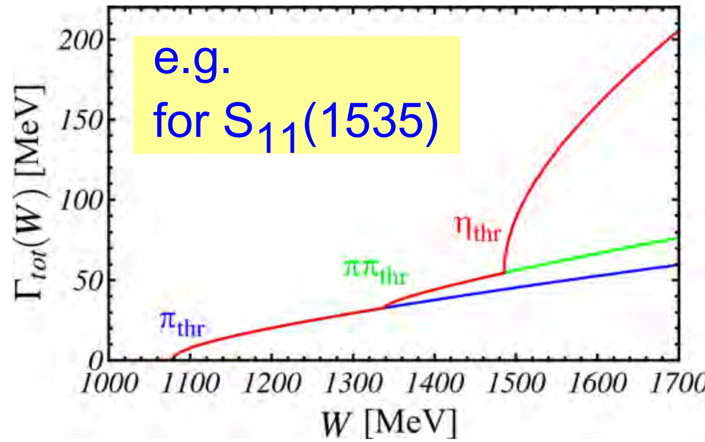

N* Resonances in EtaMAID2018 updates

Particle	J^P	overall	$N\gamma$	$N\pi$	$\Delta\pi$	$N\sigma$	$N\eta$	ΛK	ΣK	$N\rho$	$N\omega$	$N\eta'$	
N	$1/2^+$	****											
$N(1440)$	$1/2^+$	****	****	****	****	***							
$N(1520)$	$3/2^-$	****	****	****	****	**	****						
$N(1535)$	$1/2^-$	****	****	****	***	*	****						
$N(1650)$	$1/2^-$	****	****	****	***	*	****	*					
$N(1675)$	$5/2^-$	****	****	****	***	***	*	*	*				
$N(1680)$	$5/2^+$	****	****	****	****	***	*						
$N(1700)$	$3/2^-$	***	**	***	***	*	*			*			
$N(1710)$	$1/2^+$	****	****	****	*		***	**	*	*	*		
$N(1720)$	$3/2^+$	****	****	****	***	*	*	****	*	*	*		
$N(1860)$	$5/2^+$	**	*	**		*	*						
$N(1875)$	$3/2^-$	***	**	**	*	**	*	*	*	*	*		
$N(1880)$	$1/2^+$	***	**	*	**	*	*	**	**		**		
$N(1895)$	$1/2^-$	****	****	*	*	*	****	**	**	*	*	****	upgraded in 2018
$N(1900)$	$3/2^+$	****	****	**	**	*	*	**	**		*	**	
$N(1990)$	$7/2^+$	**	**	**	*	*	*	*	*				
$N(2000)$	$5/2^+$	**	**	*	**	*	*				*		
$N(2040)$	$3/2^+$	*		*									
$N(2060)$	$5/2^-$	***	***	**	*	*	*	*	*	*	*		
$N(2100)$	$1/2^+$	***	**	***	**	**	*	*		*	*	**	
$N(2120)$	$3/2^-$	***	***	***	**	**		**	*		*	*	
$N(2190)$	$7/2^-$	****	****	****	****	**	*	**	*	*	*		
$N(2220)$	$9/2^+$	****	**	****			*	*	*				
$N(2250)$	$9/2^-$	****	**	****			*	*	*				

7 N* in 2001/2003

21 N* in 2018 for γ,η

12 N* in 2018 for γ,η‘

χ^2 results for individual data sets of 4 channels

total number of data points: 10,700 - our overall χ^2/data in the fit is 2.46

		Observable	Reaction	used	W [MeV]	N	χ^2	χ^2/N	Reference
η p	5 observables	σ_0	$p(\gamma,\eta)p$	—	1488 – 1870	2880	9502	3.3	A2MAMI-17 (Run I)
		σ_0	$p(\gamma,\eta)p$	√	1488 – 1891	2712	4437	1.6	A2MAMI-17 (Run II)
		σ_0	$p(\gamma,\eta)p$	√	1888 – 1957	288	329	1.1	A2MAMI-17 (Run III)
		σ_0	$p(\gamma,\eta)p$	√	1965 – 2795	634	2276	3.6	CLAS-09
		σ_0	$p(\gamma,\eta)p$	—	1588 – 2370	680	8640	13.	CBELSA/TAPS-09
		Σ	$p(\gamma,\eta)p$	√	1496 – 1908	150	394	2.6	GRAAL-07
		Σ	$p(\gamma,\eta)p$	√	1700 – 2080	214	617	2.9	CLAS-17
		T	$p(\gamma,\eta)p$	√	1497 – 1848	144	246	1.7	A2MAMI-14
		F	$p(\gamma,\eta)p$	√	1497 – 1848	144	246	1.7	A2MAMI-14
		E	$p(\gamma,\eta)p$	√	1525 – 2125	73	155	2.1	CLAS-16
		E	$p(\gamma,\eta)p$	√	1505 – 1882	135	255	1.9	A2MAMI-17
η n	3 obs	σ_0	$n(\gamma,\eta)n$	√	1492 – 1875	880	3079	3.5	A2MAMI-14
		σ_0	$n(\gamma,\eta)n$	—	1505 – 2181	322	2986	9.3	CBELSA/TAPS-11
		Σ	$n(\gamma,\eta)n$	√	1504 – 1892	99	177	1.8	GRAAL-08
		E	$n(\gamma,\eta)n$	√	1505 – 1882	135	209	1.5	A2MAMI-17
η' p	2 obs	σ_0	$p(\gamma,\eta')p$	√	1898 – 1956	120	198	1.7	A2MAMI-17
		σ_0	$p(\gamma,\eta')p$	√	1925 – 2795	681	2013	3.0	CLAS-09
		σ_0	$p(\gamma,\eta')p$	—	1934 – 2351	200	278	1.4	CBELSA/TAPS-09
		Σ	$p(\gamma,\eta')p$	√	1903 – 1913	14	35	2.5	GRAAL-15
		Σ	$p(\gamma,\eta')p$	√	1904 – 2080	62	85	1.4	CLAS-17
η' n	1	σ_0	$n(\gamma,\eta')n$	√	1936 – 2342	170	191	1.1	CBELSA/TAPS-11

total cross sections

γ,η on **proton** and **neutron**

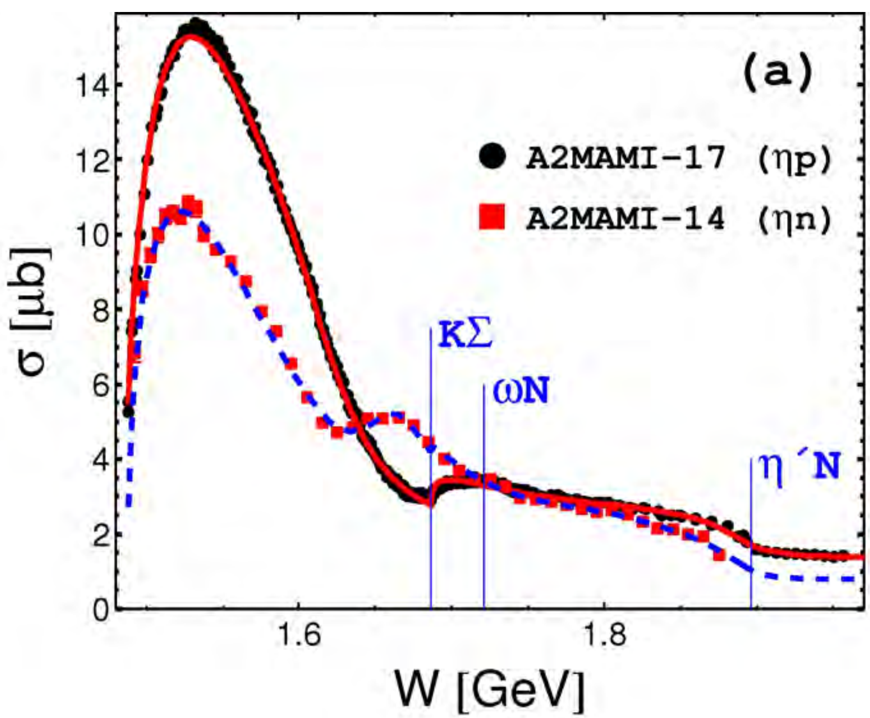

MAMI data have very high statistics and syst. errors are well under control

γ,η' on **proton** and **neutron**

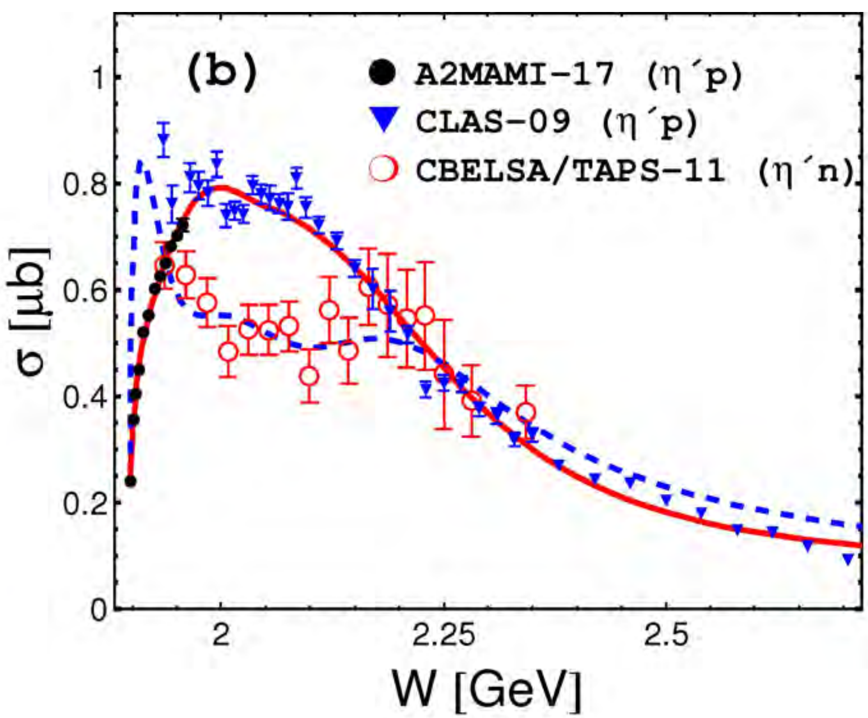

MAMI energy stops at E = 1.6 GeV
W_{max} = 1.957 GeV

total cross sections for η : bg contributions: Born + Regge

γ,η on **proton**

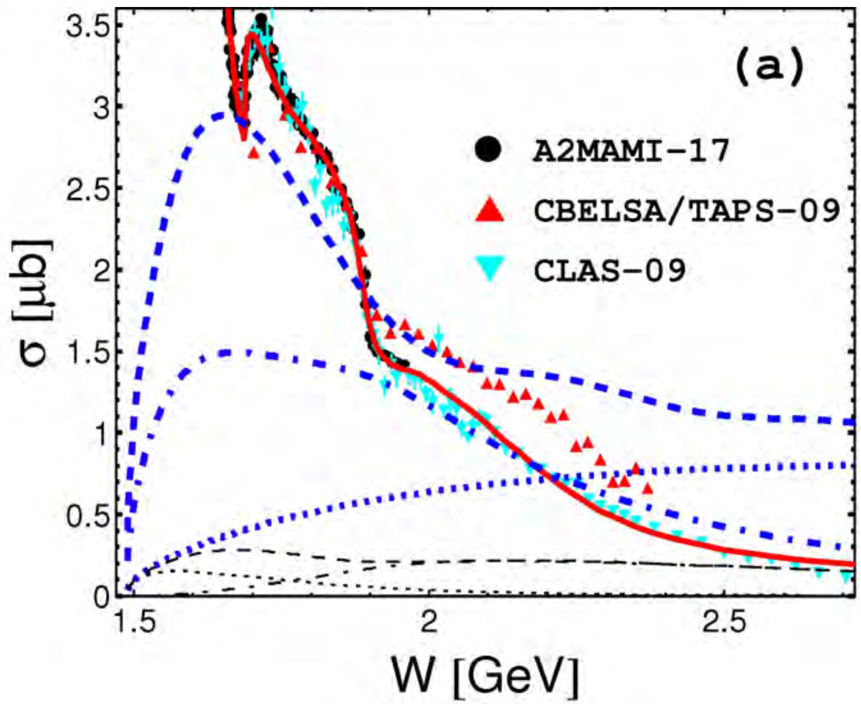

γ,η on **neutron**

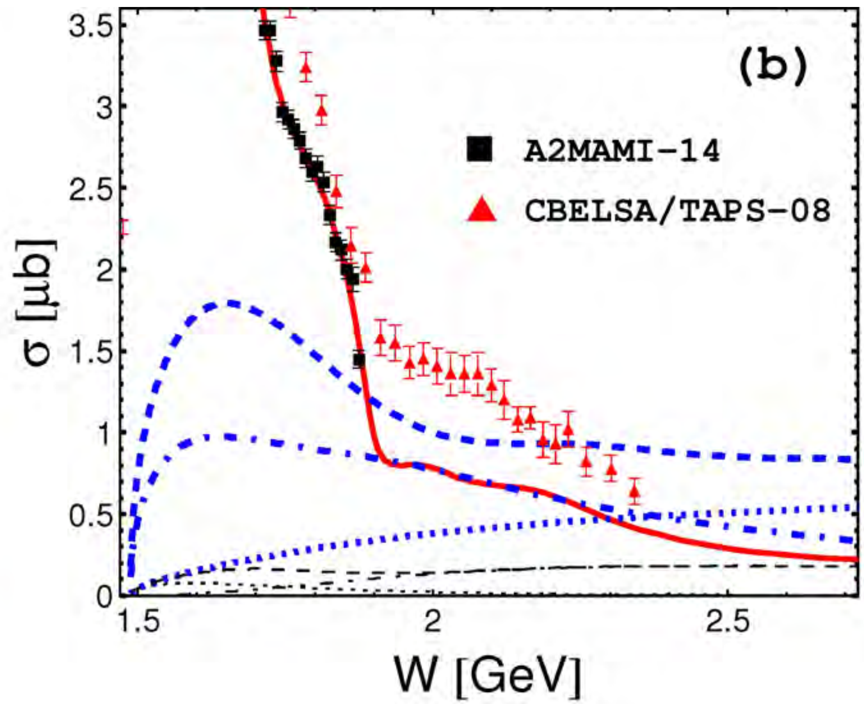

Born
Regge
Born+Regge

Born
Regge
Born+Regge
$\}$ * damping factors

total cross sections for η : Resonances and Cusps

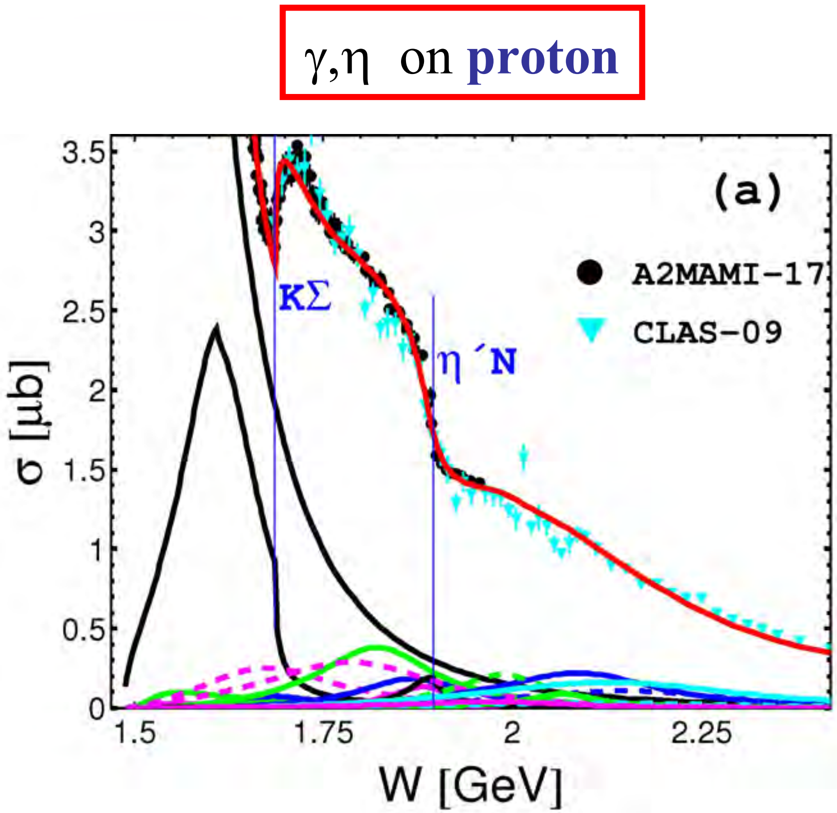

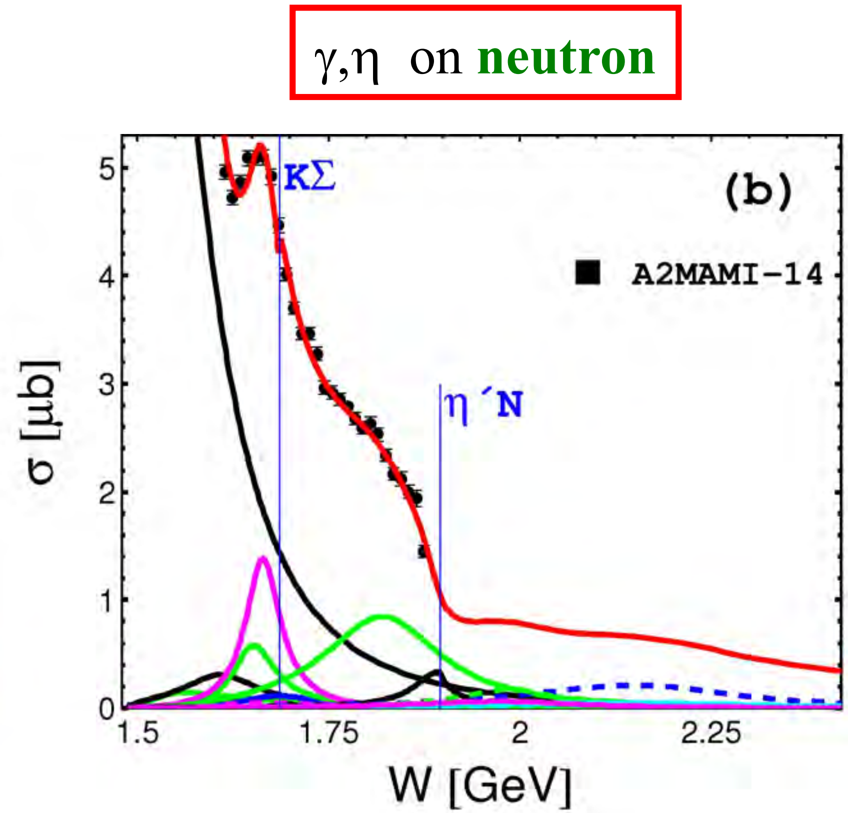

below 1.7 GeV completely dominated by S_{11}(1535)

<u>very pronounced cusp effects:</u>

S_{11}(1535) produces a cusp effect in (γ,π) at η threshold (not shown here)

S_{11}(1650) produces the cusp effect in (γ,η) at KΣ threshold

S_{11}(1895) produces the cusp effect in (γ,η) at η‘ threshold

the cusp at the η‘ threshold

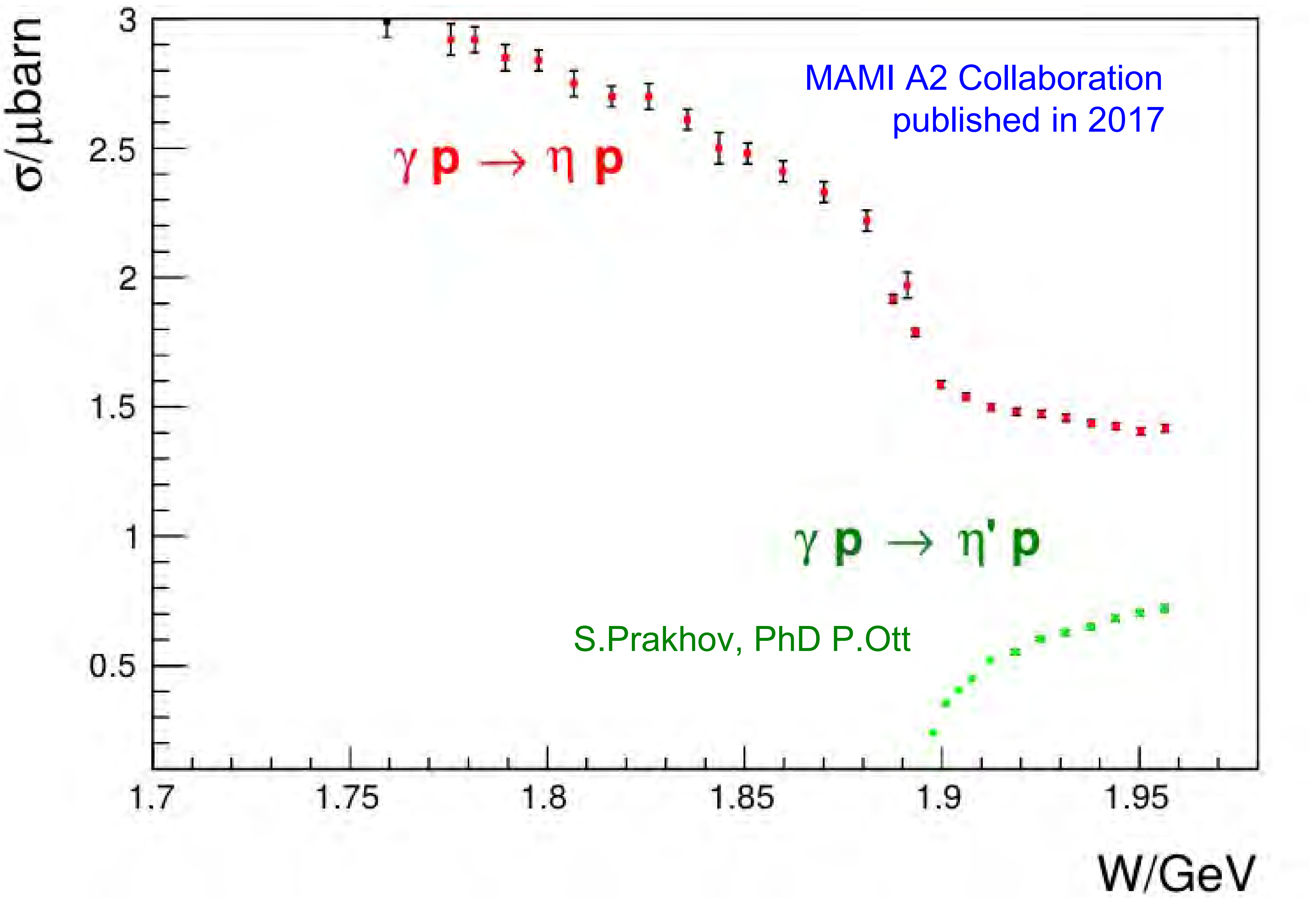

differential cross sections compared to MAMI data

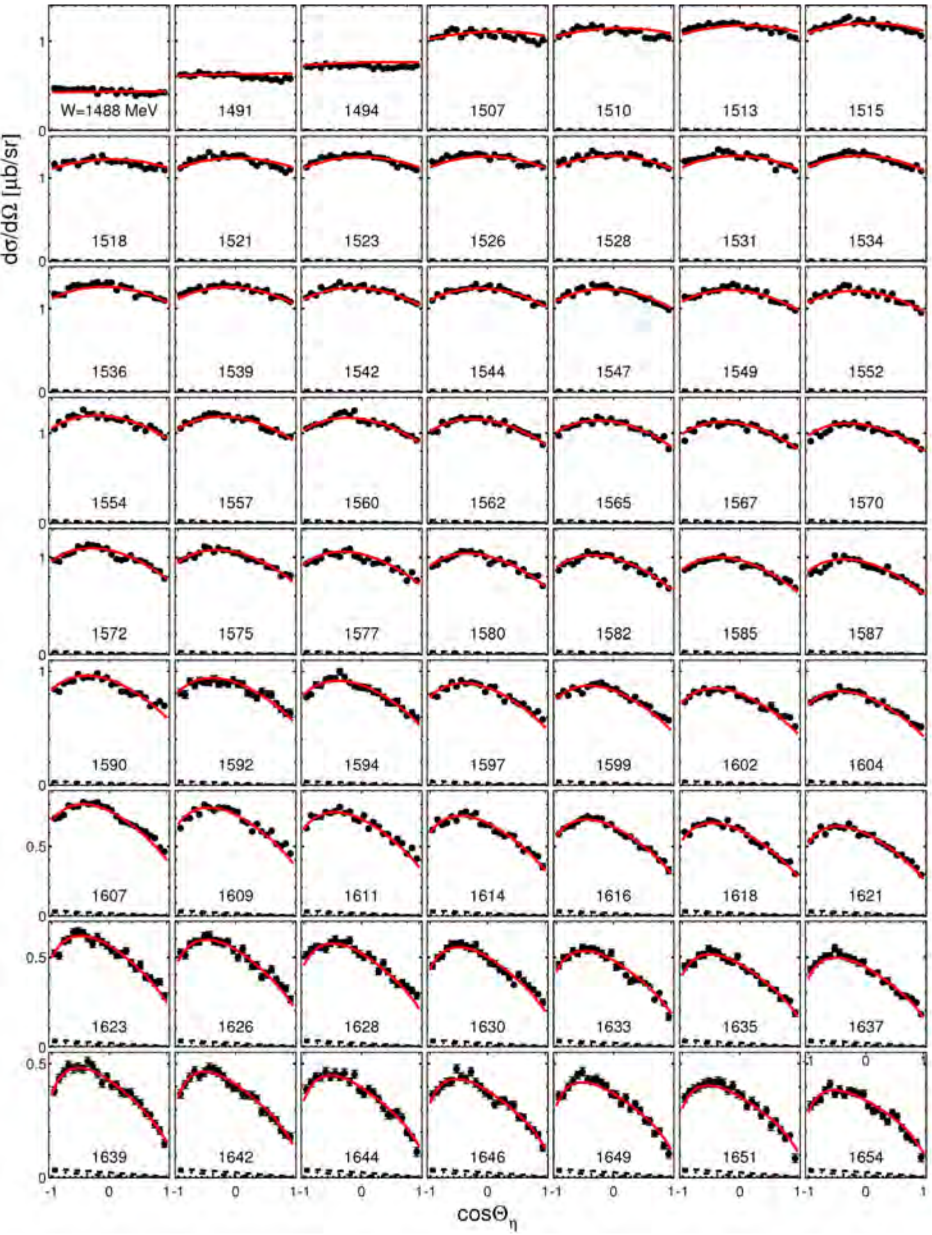

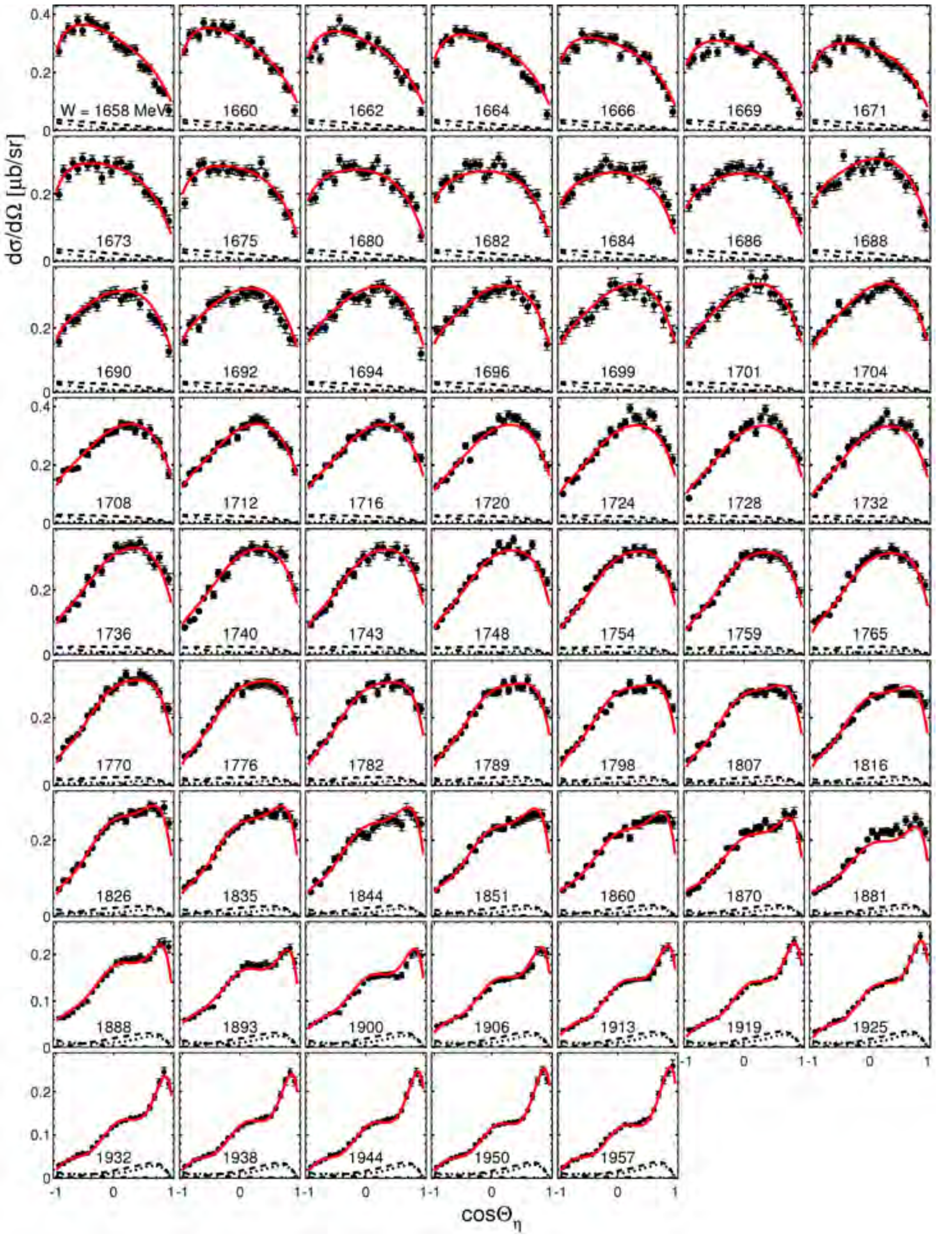

differential cross sections compared to CLAS data

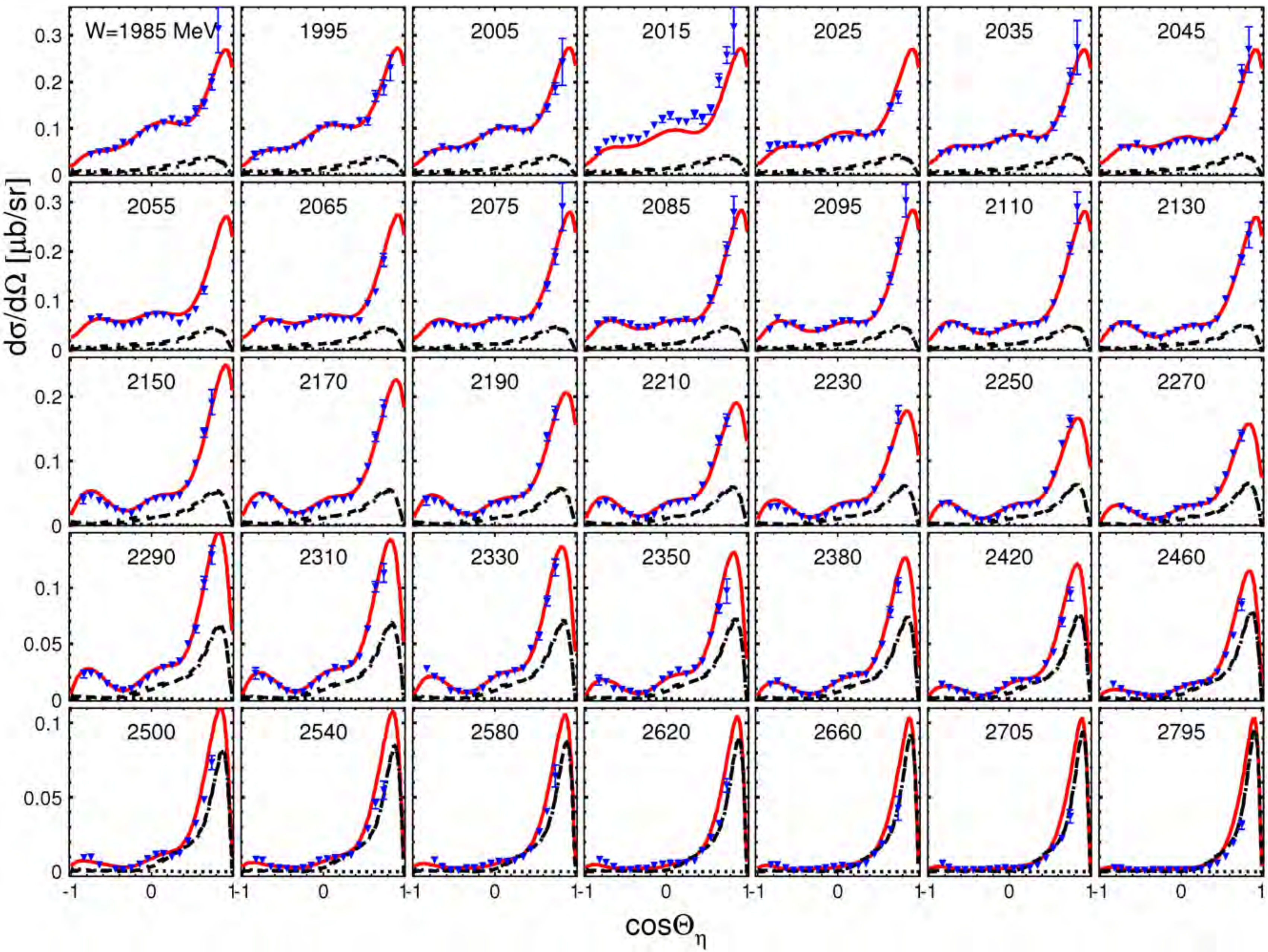

other PWA groups analyzing new (γ,η) data

BNGA: Bonn-Gatchina group:
A.V. Anisovich, E. Klempt, V.A. Nikonov, A.V. Sarantsev and U. Thoma
multi-channel K-matrix model and N/D dispersion approach

JÜBO: Jülich-Bonn group:
D. Rönchen, M. Döring, H. Haberzettl, J. Haidenbauer, U.-G. Meißner and K. Nakayama
covariant multi-channel dynamical model

KSU: Kent-State University group:
B.C. Hunt and D.M. Manley
multi-channel K-matrix model

comparison of total cross sections with other PWA

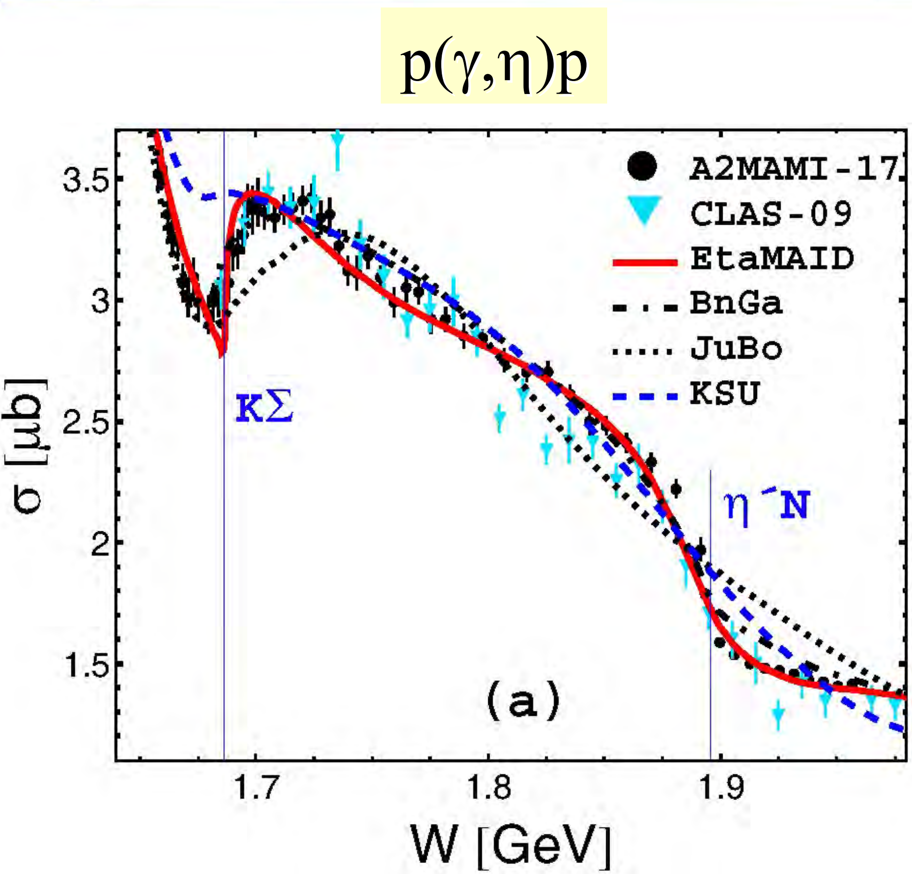

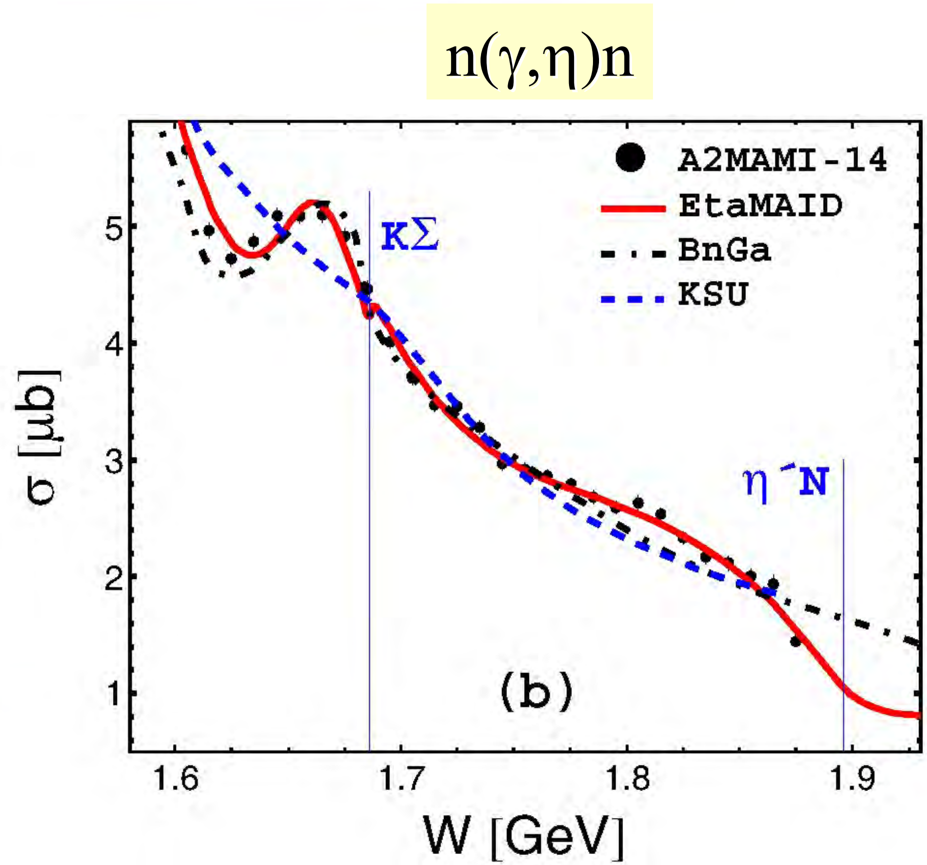

in the S11(1535) region, below W=1.6 GeV
all PWA are practically identical

also for differential cross sections
all PWA are mostly very close together

EtaMAID2018
BnGa 2018
KSU 2018
JüBo 2018

comparison with other PWA for p(γ,η)p

beam asymmetry Σ, GRAAL and CLAS data

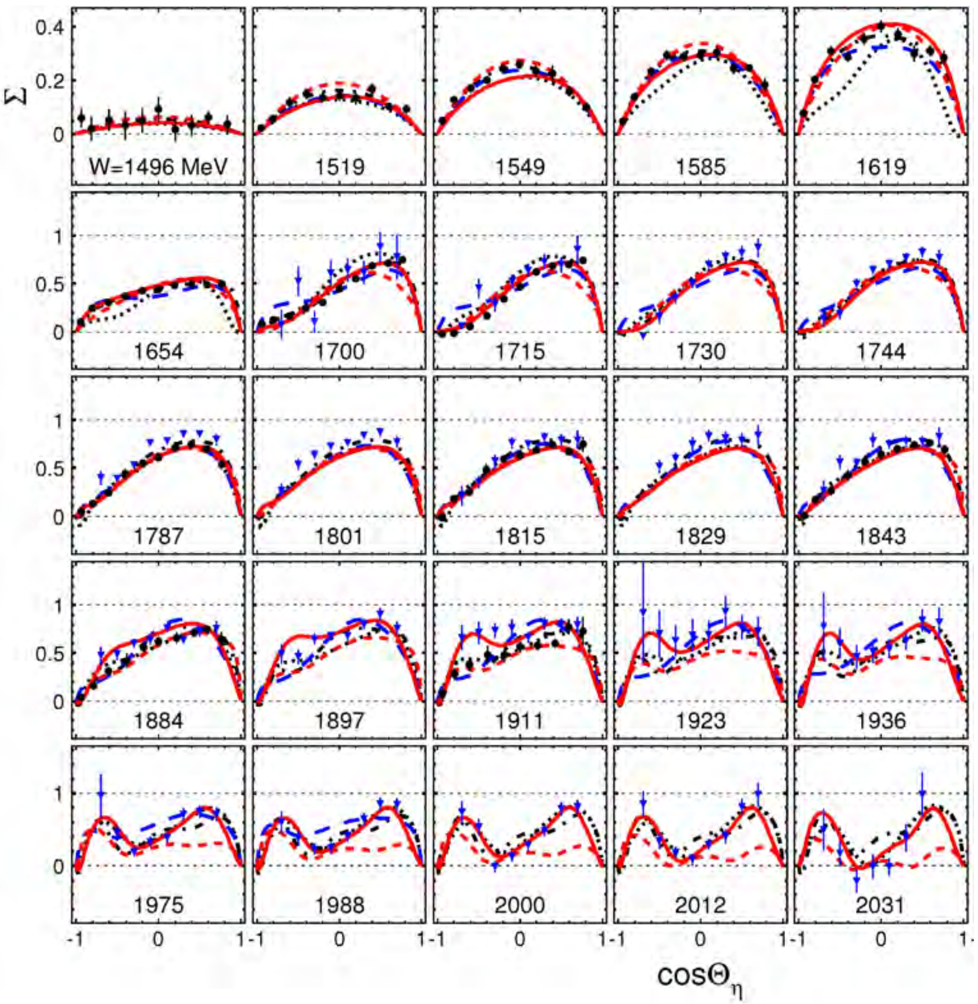

EtaMAID2018

BnGa 2018

KSU 2018

JüBo 2018

T and F asymmetries, MAMI data

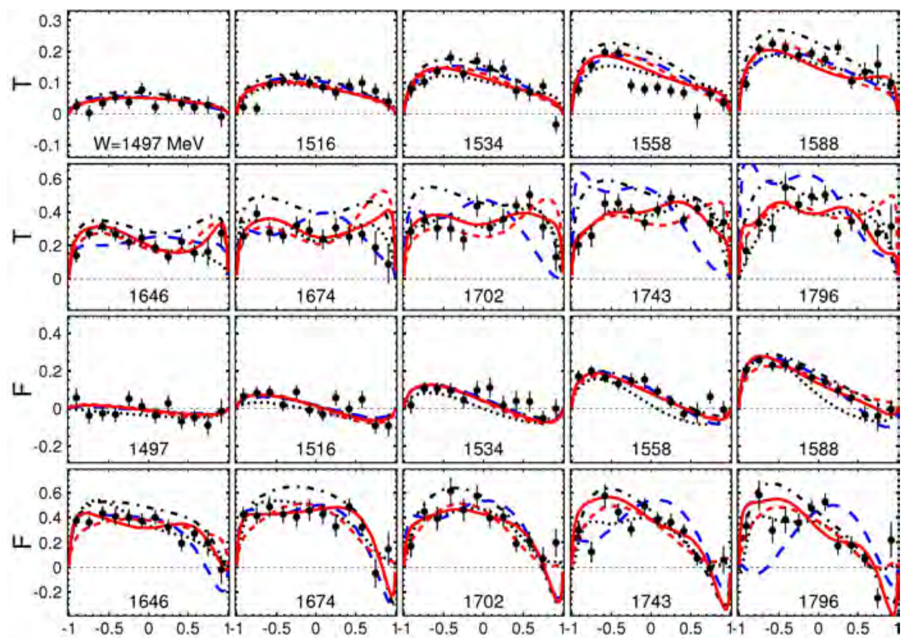

EtaMAID2015 (with single t-channel poles)

comparison with other PWA for n(γ,η)n

E asymmetry, MAMI data

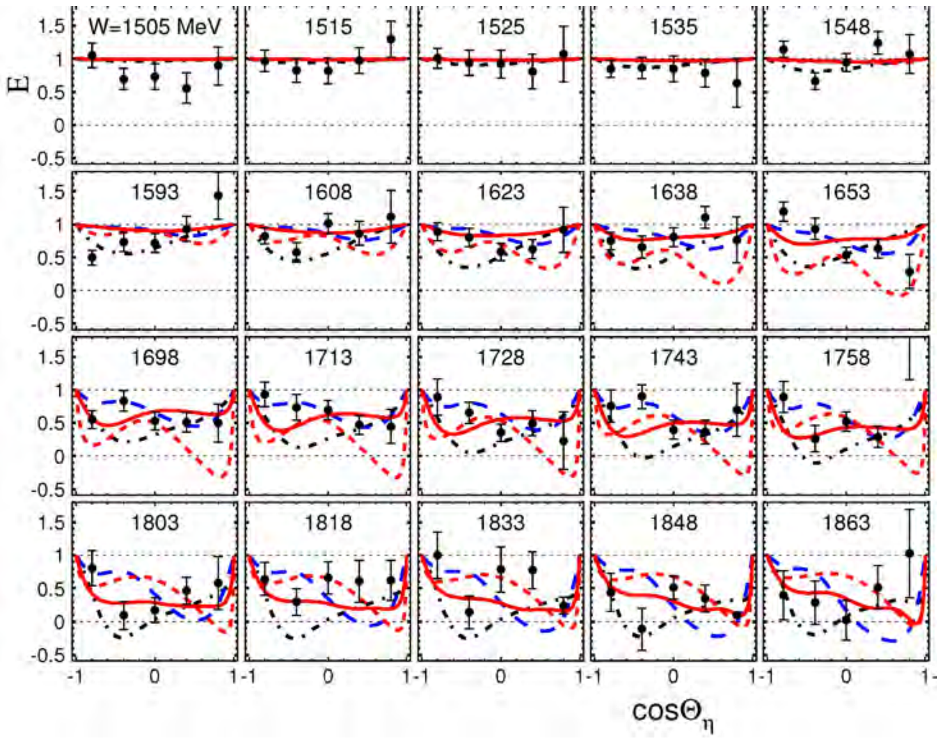

EtaMAID2018
BnGa 2018
KSU 2018

beam asymmetry Σ, GRAAL data

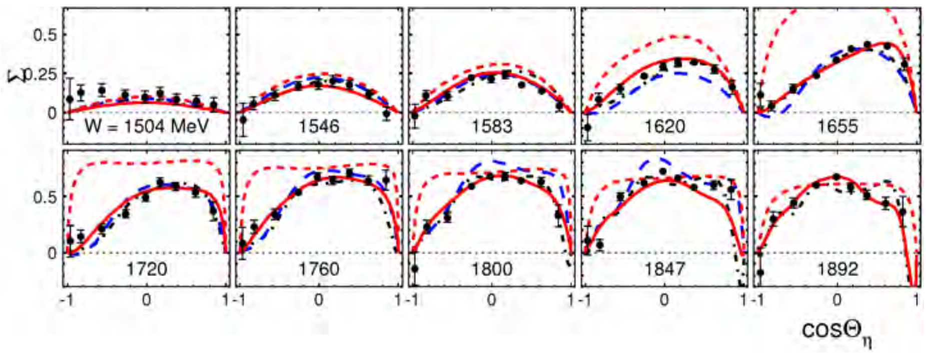

EtaMAID2015 (with single t-channel poles)

comparison of partial waves for $p(\gamma,\eta)p$

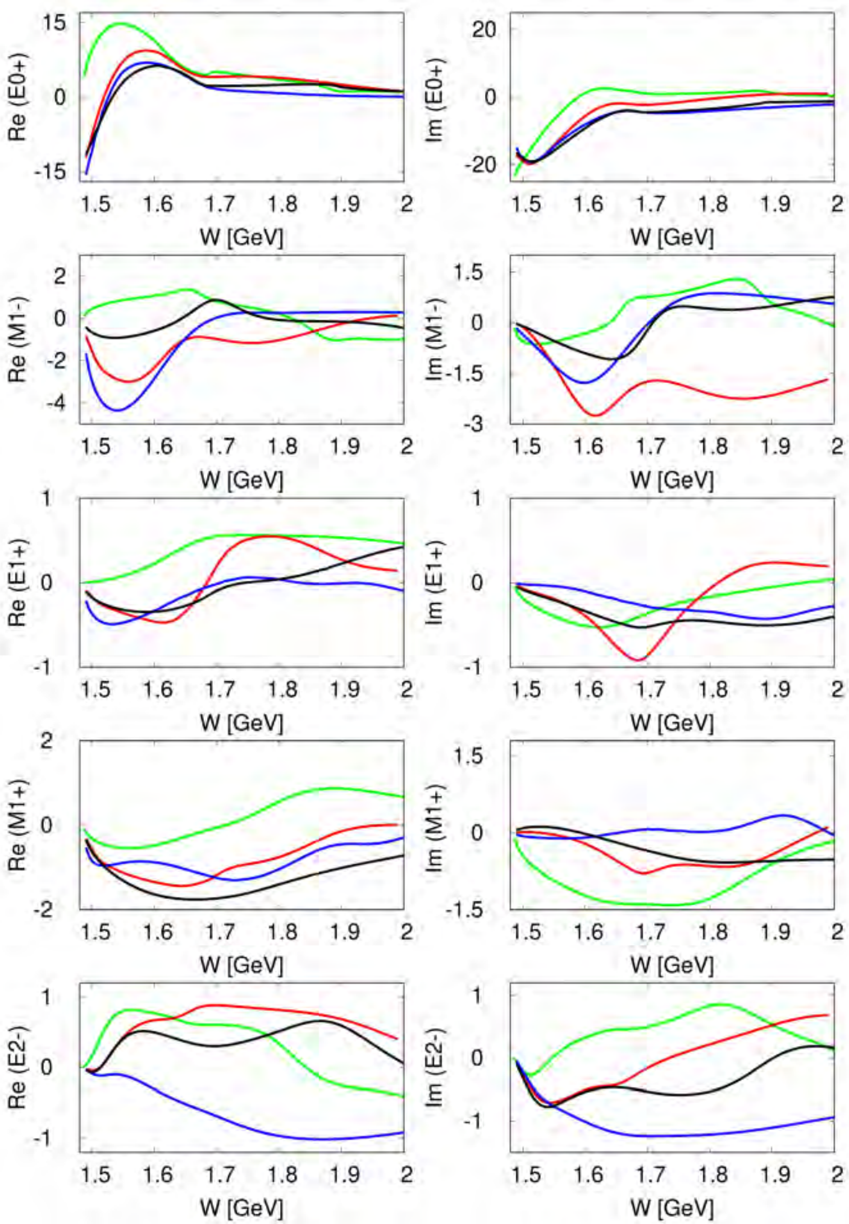

for an easier comparison, here we use the isospin convention of the other groups

$$c_{\eta N} = +1$$

EtaMAID
BnGa
JüBo
KSU

comparison of S and P waves

between new (2018) PWA

from:

our MAID solution

Bonn-Gatchina

Jülich-Bonn

Kent-State

phase issues

our newly introduced unitarity phase Φ
for each resonance contribution
spoils the agreement with other PWA, even for the S wave

$$t^{\alpha}_{\gamma,\eta}(W) = t^{\alpha,Born}_{\gamma,\eta}(W) + t^{\alpha,VM(Regge)}_{\gamma,\eta}(W) \cdot F_d(W)$$

$$+ \sum_{j=1}^{N_\alpha} t^{\alpha,BW,j}_{\gamma,\eta}(W) \cdot e^{i\Phi_j}$$

phenomenological phase
taken as a free parameter

e.g. for the ηp channel and S11(1535): $\Phi = 20°$

comparison of partial waves after phase rotation for p(γ,η)p

comparison of S and P waves

between new (2018) PWA

from:

our MAID solution

Bonn-Gatchina

Jülich-Bonn

Kent-State

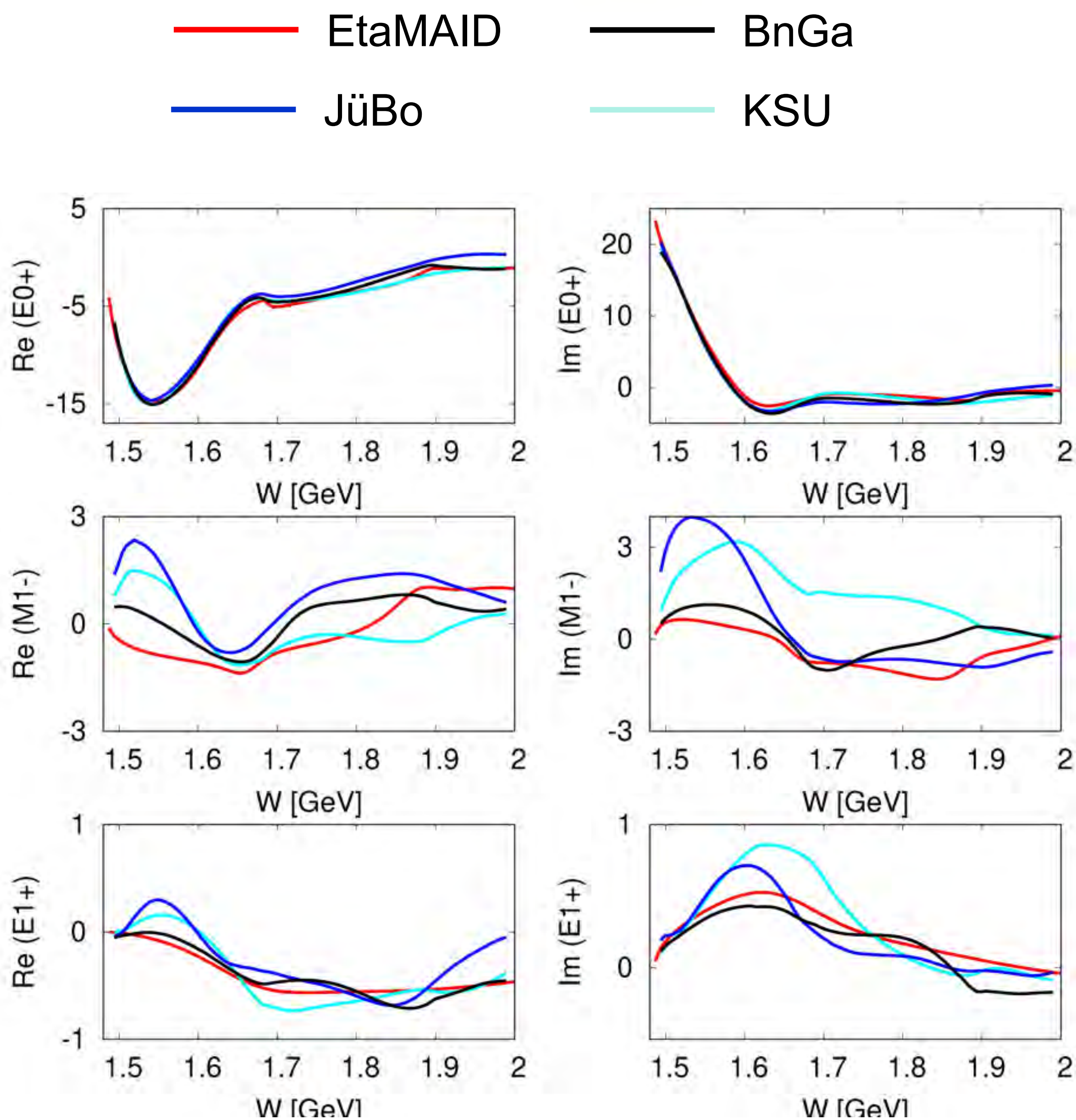

S waves are almost identical

some higher pw are close

other pw differ a lot,

due to incomplete experiments!

predictions for unmeasured polarization observables

EtaMAID — BnGa — JüBo — KSU

beam-target H

recoil pol. P
equivalent to beam-target

beam-target G

beam-recoil $C_{x'}$
very hard

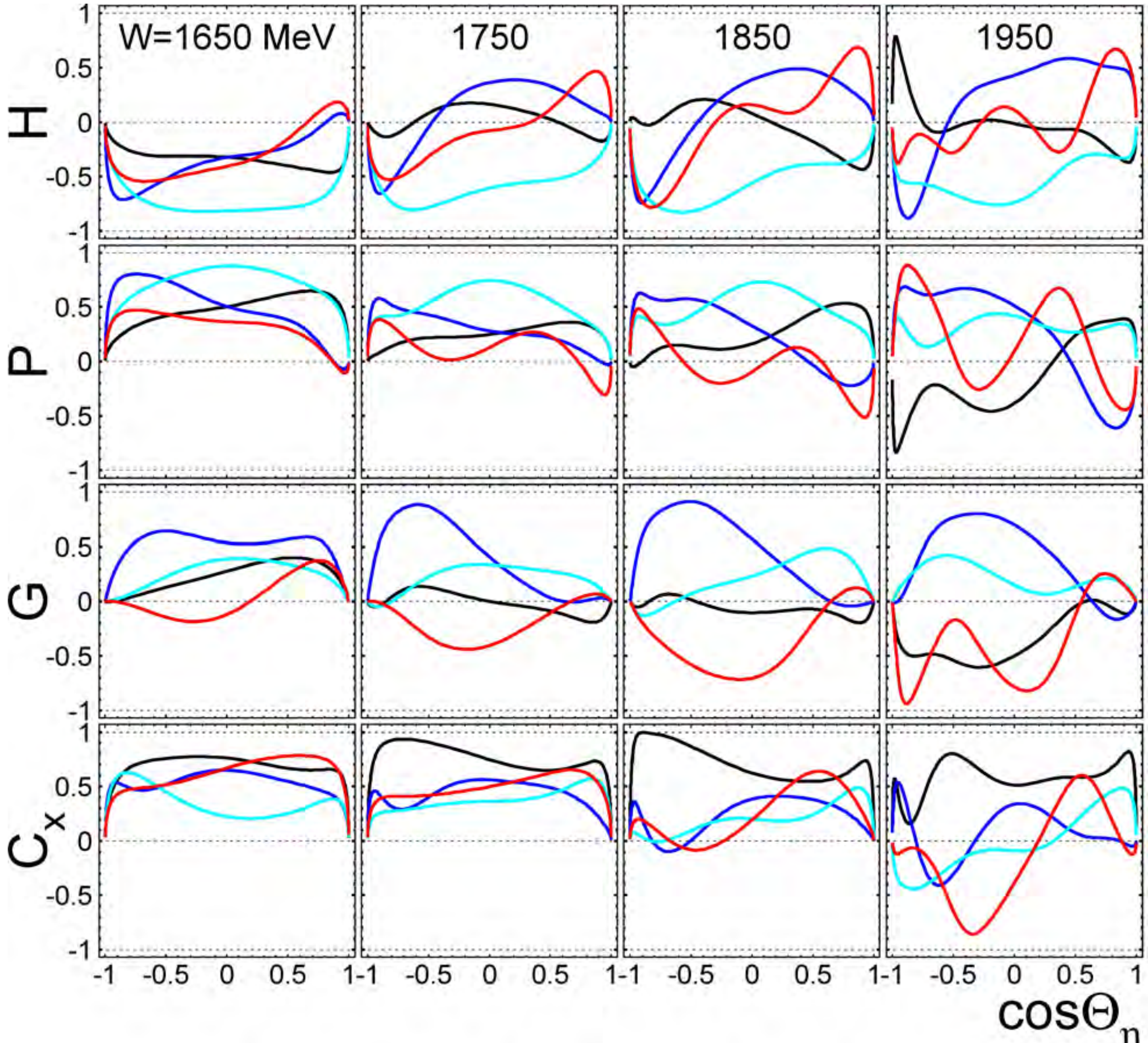

error analysis for Breit-Wigner parameters of selected N*

in total we have 21 N* resonances contributing to η photoproduction (8 of them also to γ,η')

Table 4. Breit-Wigner parameters for selected resonances: mass M_{BW}, total width Γ_{BW}, branching ratio $\beta_{\eta N}$ to ηN, and helicity amplitudes $A_{1/2}^{p(n)}$ for proton (neutron). The first row for each resonance gives a parameter set of the presented EtaMAID solution. The parameters indicated without errors were fixed during the fit. The second row indicate an overall status of the resonance and lists the corresponding parameters estimated by PDG [1] (NE means "No Estimates" given by PDG). The effective $\eta' N$ branching ratios according to ref. [75] for the $N(1880)1/2^+$ and $N(1895)1/2^-$ are $(6.3 \pm 2)\%$ and $(19.5 \pm 5)\%$, respectively.

Resonance J^P	M_{BW} [MeV]	Γ_{BW} [MeV]	$\beta_{\eta N}$ [%]	$A_{1/2}^p$ $[10^{-3}\,\mathrm{GeV}^{-1/2}]$	$A_{1/2}^n$ $[10^{-3}\,\mathrm{GeV}^{-1/2}]$
$N(1535)1/2^-$	1522 ± 8	175 ± 25	34 ± 5	$+115$	-102 ± 8
$****$	1530 ± 15	150 ± 25	42 ± 13	$+105 \pm 15$	-75 ± 20
$N(1650)1/2^-$	1626^{+10}_{-5}	133 ± 20	19 ± 6	$+55$	-25 ± 20
$****$	1650 ± 15	125 ± 25	25 ± 10	$+45 \pm 10$	-10^{+40}_{-30}
$N(1710)1/2^+$	1670 ± 20	63^{+55}_{-18}	12 ± 4	5.5	-42^{+16}_{-12}
$****$	1710 ± 30	140 ± 60	30 ± 20	NE	NE
$N(1880)1/2^+$	1882 ± 24	90^{+70}_{-30}	43^{+10}_{-20}	60	-7^{+60}_{-60}
$***$	1880 ± 50	300 ± 100	NE	NE	NE
$N(1895)1/2^-$	1894.4^{+5}_{-15}	71^{+25}_{-13}	3.3 ± 1.5	-32	$+43^{+30}_{-50}$
$****$	1895 ± 25	120^{+80}_{-40}	25^{+15}_{-10}	NE	NE

However, our goal for nucleon resonance analysis is
to get the pole positions and residues
and error analysis for these more fundamental N* properties.

comparison of pole positions and residues from EtaMAID2018

obtained by analytical continuation into the 2nd Riemann sheet

		mass	width	pole mass	pole width	ResE	θ_E	ResM	θ_M
1.000	S11(1535) [1]	1.522	0.175	1.477	0.165	1971.000	20.561	0.000	0.000
2.000	S11(1650)	1.626	0.132	1.614	0.131	350.750	-175.710	0.000	0.000
3.000	S11(1895)	1.894	0.071	1.892	0.070	47.641	-129.060	0.000	0.000
4.000	P11(1440) [1]	1.430	0.350	1.361	0.168	0.000	0.000	499.710	-86.314
5.000	P11(1710)	1.669	0.063	1.663	0.060	0.000	0.000	16.854	120.400
6.000	P11(1880)	1.882	0.090	1.876	0.088	0.000	0.000	37.105	-100.290
7.000	P11(2100)	2.010	0.260	1.979	0.249	0.000	0.000	126.900	-98.076
8.000	P13(1720)	1.750	0.396	1.660	0.251	68.442	56.459	81.154	56.459
9.000	P13(1900)	1.899	0.450	1.816	0.304	14.262	27.064	205.840	27.064
10.000	D13(1520)	1.520	0.100	1.506	0.088	38.581	-13.435	25.411	-13.435
11.000	D13(1700)	1.660	0.084	1.650	0.076	3.338	-137.200	8.623	-137.200
12.000	D13(1875)	1.894	0.320	1.824	0.188	63.328	-177.780	56.235	-177.780
13.000	D13(2120)	2.061	0.102	2.056	0.101	28.208	-30.110	1.527	149.890
14.000	D15(1675)	1.680	0.100	1.669	0.094	1.948	-117.880	10.620	-117.880
15.000	D15(2060)	1.984	0.160	1.969	0.154	6.412	-117.730	30.977	62.266
16.000	D15(2570) [2]	0.000	0.000	0.000	0.000	0.000	0.000	0.000	0.000
17.000	F15(1680)	1.690	0.145	1.669	0.128	15.148	36.445	11.791	36.445
18.000	F15(1860)	1.886	0.197	1.857	0.175	4.823	78.145	23.944	78.145
19.000	F15(2000)	2.117	0.247	2.086	0.229	36.526	76.611	25.571	-103.390
20.000	F17(1990)	2.227	0.389	2.166	0.344	22.243	171.650	24.098	-8.354
21.000	G17(2190)	2.250	0.591	2.127	0.439	51.613	66.306	9.796	66.306
22.000	G19(2250)	2.250	0.733	2.085	0.478	4.854	-126.730	18.158	-126.730
23.000	H19(2220) [2]	0.000	0.000	0.000	0.000	0.000	0.000	0.000	0.000

masses and widths in GeV, multipole residues in units of MeV mfm , phase in °

[1] pole mass below threshold (on different RS) [2] no sensitivity found for this resonance

And in order to get less or even in-dependent of the models, we are now generating single-energy partial waves, which we then analyze with the L+P method.

single-energy analysis
with
analytical constraints

Fixed-t analyticity as a constraint in single-energy partial-wave analyses of meson photoproduction reactions,

Phys Rev C97 (2018) 015207

single-energy (SE-4) vs energy-dependent (ED) PWA for p(γ,η)p

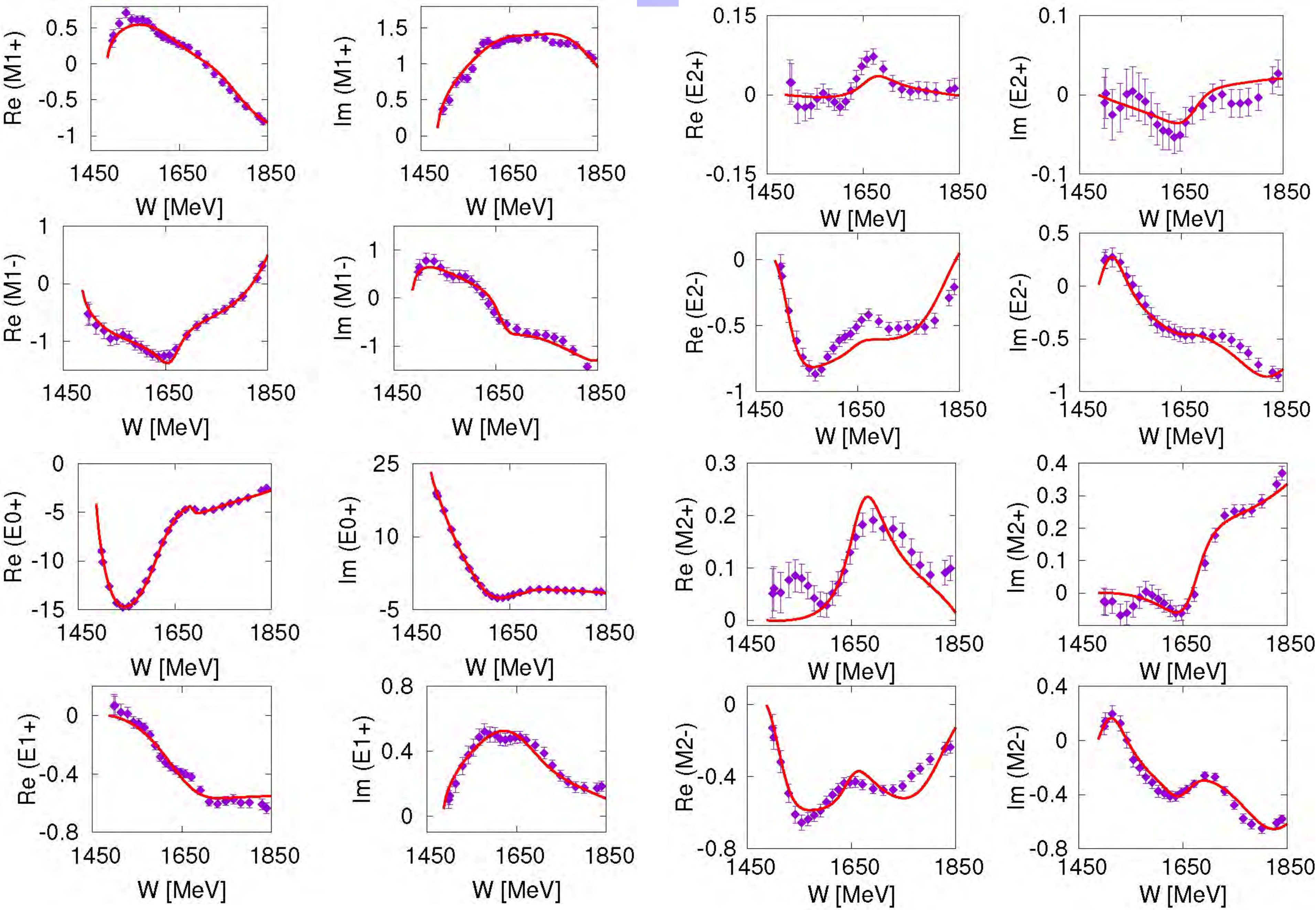

single-energy (SE-4) vs energy-dependent (ED) PWA for p(γ,η)p

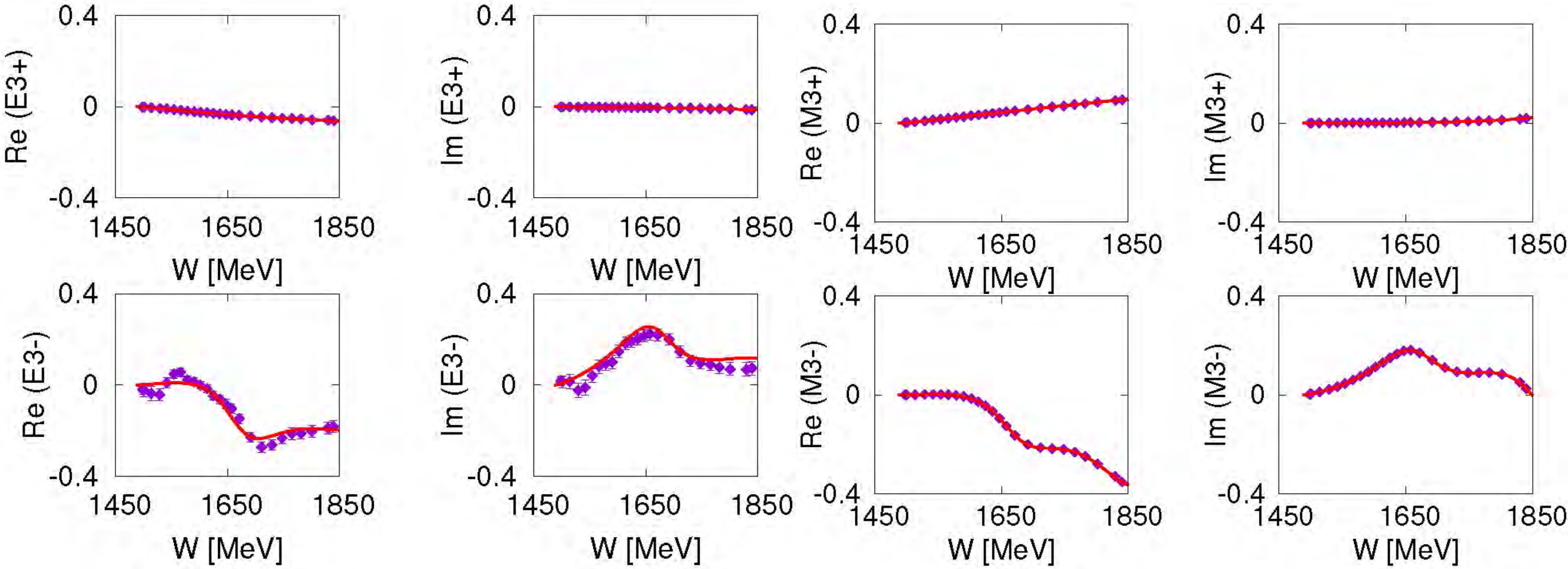

in SE-4 only 9 multipoles have been freely fitted,

M3- was kept constant as all other higher multipoles

comparison of pole positions

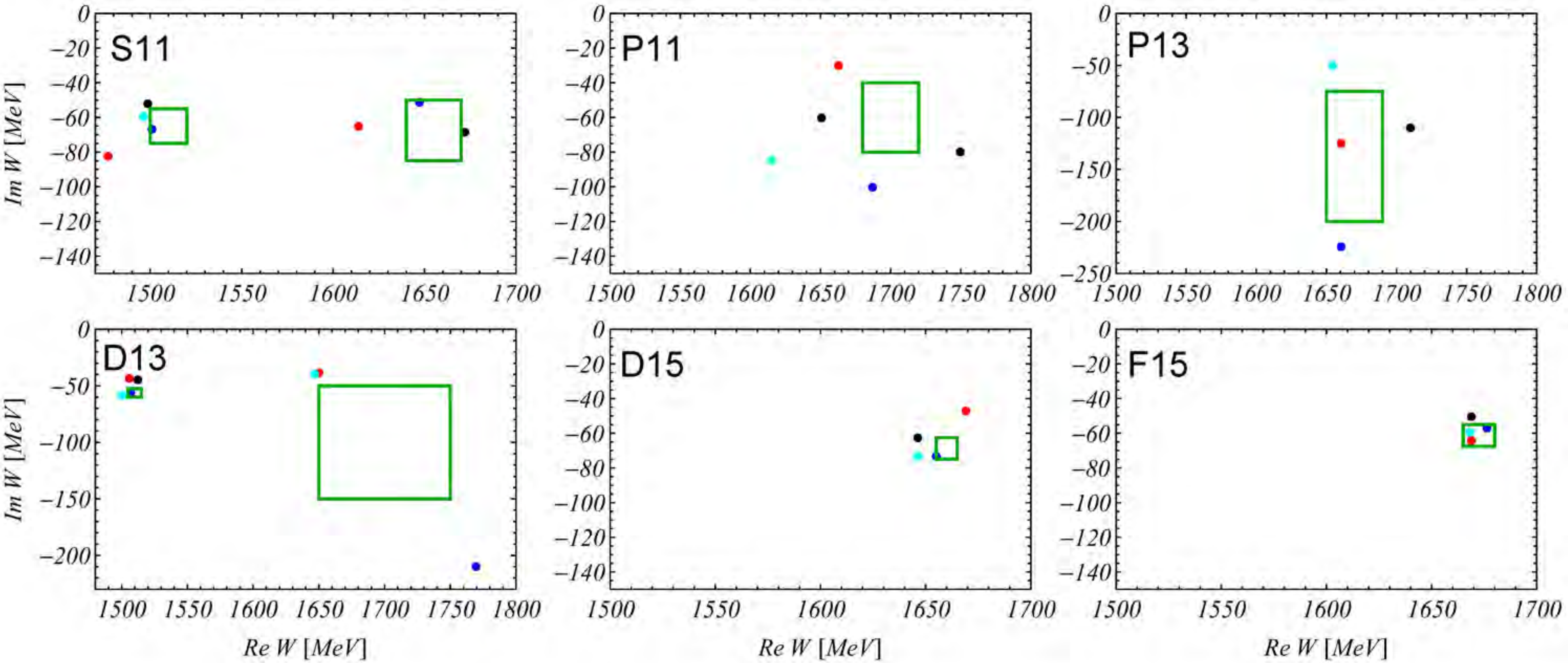

PDG ranges

EtaMAID
BnGa
JüBo
KSU

comparison of pole positions and residues

EtaMAID and JüBo by analytical continuation

	EtaMAID 2018	JüBo 2017	BoGa 2018
S11(1535) **E0+**	1477 – 165/2 i 1971, 21°	1495 – 112/2 i 736, 149°	see
S11(1650) **E0+**	1614 – 131/2 i 351, –176°	1674 – 130/2 i 102, 57°	Andrey‘s
D13(1520) **E2 –** **M2 –**	1506 – 88/2 i 38.6, –13° 25.4, –13°	1509 – 98/2 i 13.4, 123° 10.4, 108°	talk
D15(1675) **E2+** **M2+**	1669 – 94/2 i 1.95, –118° 10.6, –118°	1647 – 135/2 i 3.7, 59° 22.6, –31°	from
F15(1680) **E3 –** **M3 –**	1669 – 128/2 i 15.1, 36° 11.8, 36°	1666 – 80/2 i 2.9, 126° 1.7, 125°	this morning

in most cases, the residues disagree completely with each others

comparison of pole positions and residues

	EtaMAID 2018	JüBo 2017	
D13(1700)	1650 – 76/2 i		
E2 –	3.3, –137°		
M2 –	8.6, –137°		
P11(1710)	1663 – 60/2 i	1731 – 157/2 i	1750 – 316/2 i *)
M1 –	16.9, 120°	14.7, –85°	57.0, 161°
P13(1720)	1660 – 251/2 i	1689 – 190/2 i	
E1+	68.4, 56°	3.7, –165°	
M1+	81.2, 56°	3.3, –90°	

*) JüBo has 2 poles in P11 partial wave,
the pole masses are too close for a separation with data on the real axis

in most cases, the residues disagree completely with each others

simplified P11 map of JüBo model

no bg is added

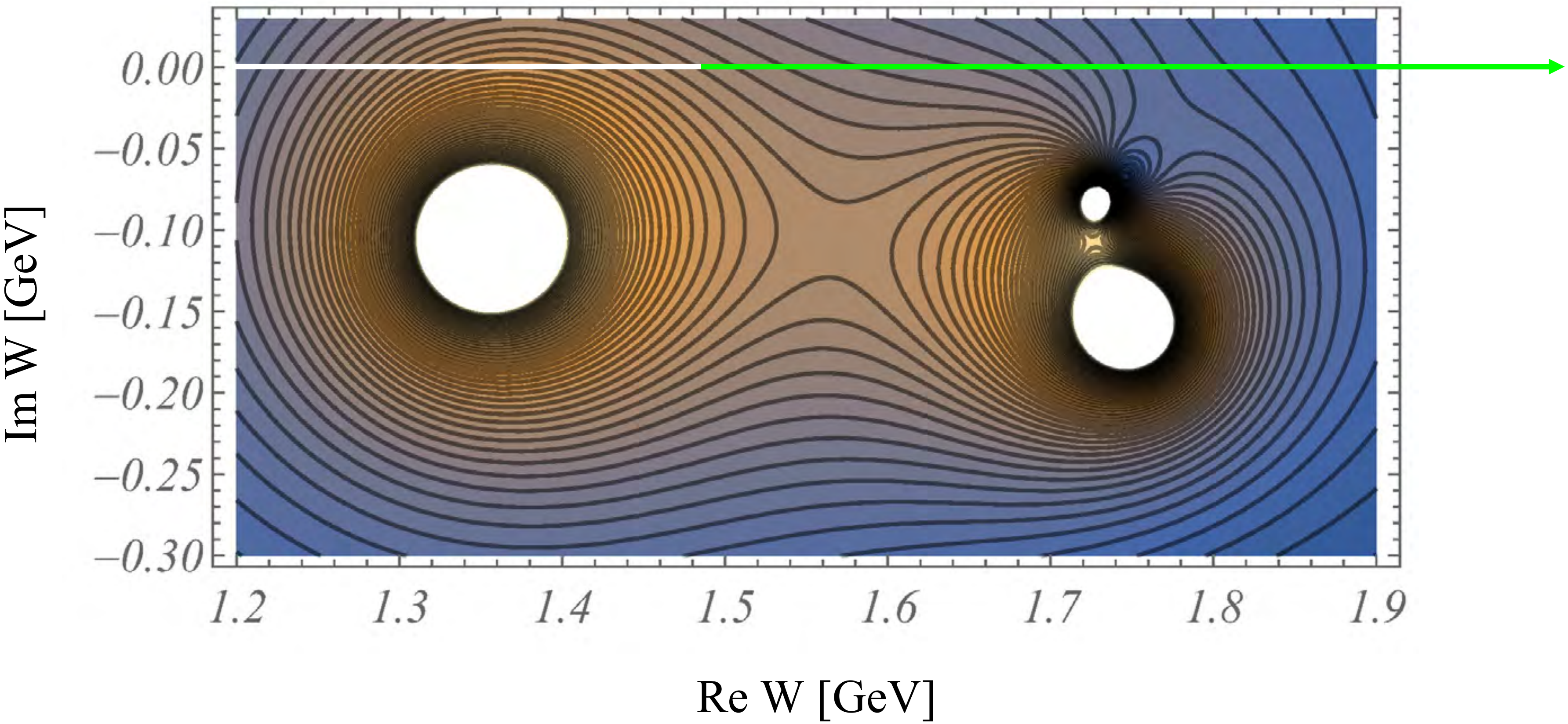

such a situation is too difficult for L+P

summary and conclusions

EtaMAID2018 describes all data of 4 channels ηp, ηn, η'p, η'n very well,

In comparison of MAID with BnGa, JüBo, KSU we find that all PWAs describe the $\gamma + p$ --> η + p similarly well, but the partial waves are besides the dominant S wave E0+ very different.

The reason can be:

1) the experiment is not complete,
   some polarization observables are still missing

2) an overall phase is undetermined
   and the phase can even be angle-dependent

3) in EtaMAID unitarity constraints are weak or even missing
   unlike pion photoproduction, where the Watson Theorem is a very strong unitarity constraint

total cross sections for η‘ : Resonances and Cusps

γ,η‘ on **proton**

γ,η‘ on **neutron**

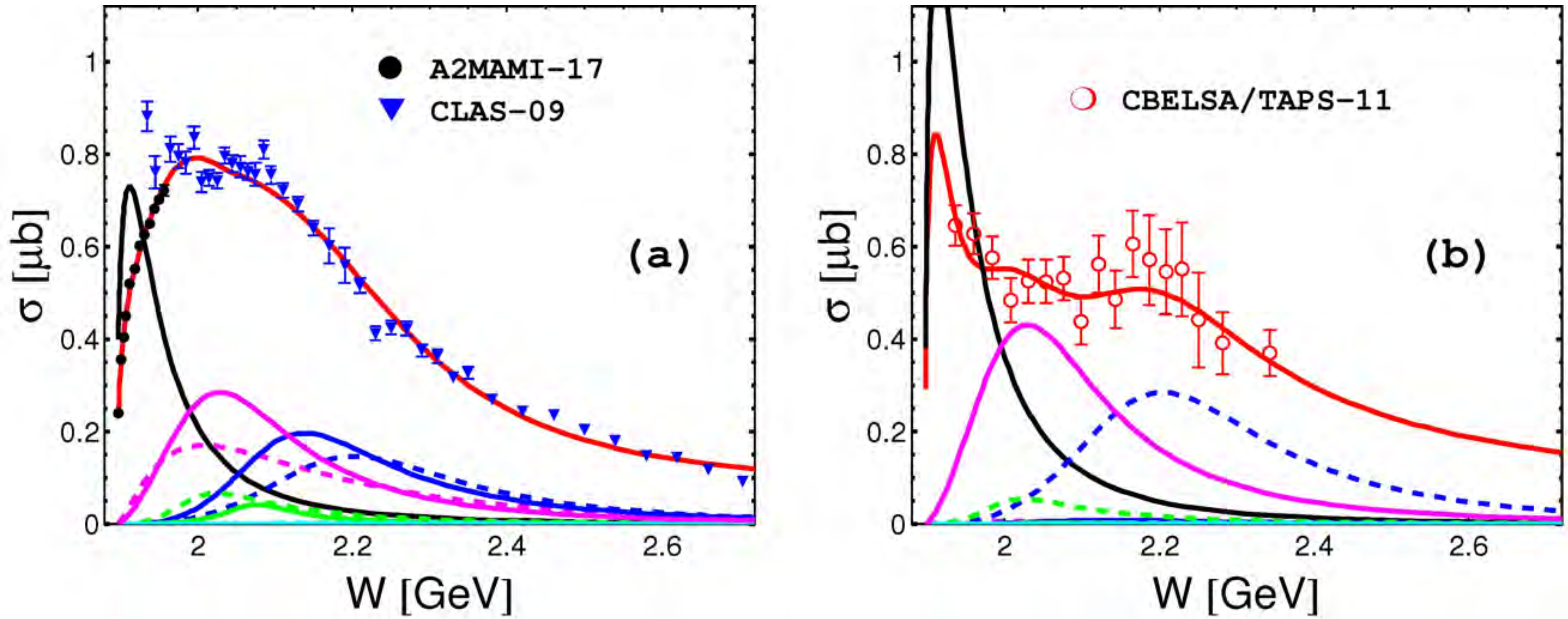

dominant resonance contributions found in η‘ with EtMAID2018

N(1895)1/2⁻ **S$_{11}$** : M_{BW} = 1894.4 MeV (1.6 MeV below η‘ thresh)

N(2100)1/2⁺ **P$_{11}$** : M_{BW} = 2010 MeV

N(1900)3/2⁺ **P$_{13}$** : M_{BW} = 1899 MeV

N(2000)5/2⁺ **F$_{15}$** : M_{BW} = 2117 MeV

N(1990)7/2⁺ **F$_{17}$** : M_{BW} = 2227 MeV

from Andrey Sarantev's talk at Meson2018:

The analysis of the $\gamma p \to \eta' p$ data.

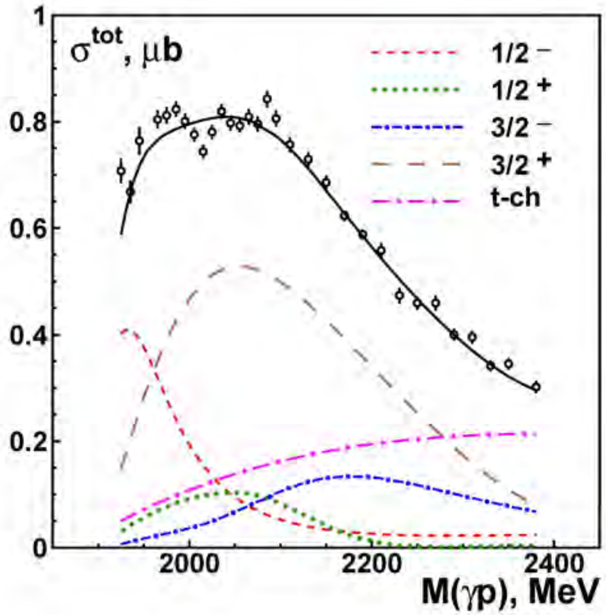

very different resonance contributions!
(for γ,η we are much more similar)

the reason for that is:

large ambiguity in PWA solutions
due to very incomplete experiments
in etaprime production

only 2 observables: $d\sigma/d\Omega$ and Σ
have been measured

Strong contribution from the $S_{11}(1895)$, $P_{13}(1900)$, $P_{11}(2100)$ and $D_{13}(2120)$ states.

with EtaMAID2018 we find strongest contributions for $S_{11}(1895)$, $P_{11}(2100)$ and $F_{15}(2000)$